

# Spitzer/IRS spectroscopy of high mass precursors to planetary nebulae

D. A. García-Hernández<sup>1</sup>, J. V. Perea-Calderón<sup>2</sup>, M. Bobrowsky<sup>3</sup> and P. García-Lario<sup>4</sup>

## ABSTRACT

We present Spitzer/IRS observations of a small sample of heavily obscured IRAS sources displaying both the infrared and OH maser emission characteristic of OH/IR stars on the asymptotic giant branch (AGB), but also radio continuum emission typical of ionized planetary nebulae (PNe), the so-called *OHPNe*. Our observations show that their mid-infrared spectra are dominated by the simultaneous presence of strong and broad amorphous silicate absorption features together with crystalline silicate features, originated in their O-rich circumstellar shells. Out of the five sources observed, three of them are clearly non-variable at infrared wavelengths, confirming their post-AGB status, while the remaining two still show strong photometric fluctuations, and may still have not yet departed from the AGB. One of the non-variable sources in the sample, IRAS 17393–2727, displays a strong [Ne II] nebular emission at 12.8  $\mu\text{m}$ , indicating that the ionization of its central region has already started. This suggests a rapid evolution from the AGB to the PN stage. We propose that these heavily obscured OHPNe represent the population of high mass precursors to PNe in our Galaxy.

*Subject headings:* stars: AGB and post-AGB — circumstellar matter — dust, extinction — planetary nebulae: general — infrared: stars

---

<sup>1</sup>The W. J. McDonald Observatory. The University of Texas at Austin. 1 University Station, C1400. Austin, TX 78712–0259, USA; agarcia@astro.as.utexas.edu

<sup>2</sup>European Space Astronomy Centre, INSA S. A., P.O. Box 50727. E-28080 Madrid. Spain; Jose.Perea@sciops.esa.int

<sup>3</sup>Computer Sciences Corporation/Space Telescope Science Institute. Baltimore MD, USA; matt@mailaps.org

<sup>4</sup>Herschel Science Centre. European Space Astronomy Centre, Research and Scientific Support Department of ESA. Villafranca del Castillo, P.O. Box 50727. E-28080 Madrid. Spain; Pedro.Garcia-Lario@sciops.esa.int

## 1. Introduction

The evolution of low- and intermediate-mass stars ( $1-8 M_{\odot}$ ) ends with a strong mass loss phase at the tip of the asymptotic giant branch (AGB) and the subsequent formation of a new planetary nebula (PN) (e.g. Kwok 2000). The transition time required for an AGB star to become a PN (the so-called “post-AGB” phase) depends essentially on the initial mass of the progenitor star, and it ranges from just a few hundred years for the most massive stars, to several thousand years for low mass progenitors (e.g. Bloeker 1995). Crucial changes affecting both the morphology and the chemistry of the central star also occur during this short-lived post-AGB phase which completely determine the subsequent evolution of the star as a PN (see e.g. van Winckel 2003).

Most candidate post-AGB stars were identified as such now more than 20 years ago, based on the infrared photometry provided by IRAS, as these stars show characteristic infrared colours (e.g. García-Lario et al. 1997, and references therein). However, the confirmation of their post-AGB nature has only been systematically explored more recently, through extensive ground-based follow-up spectroscopic surveys in the optical (García-Lario 2006, and references therein). As a consequence of this, a few hundred candidates have been identified as genuine post-AGB stars (e.g. Suárez et al. 2006). However, it is suspected that a strong bias exists in the type of stars identified this way since they may only represent the slowly evolving, low-mass population of post-AGB stars in the Galaxy. These low-mass stars experience lower mass loss rates at the end of the AGB phase and thus are more easily detectable in the optical as bright stars of intermediate spectral type. In contrast, very little is known about the population of more massive, heavily obscured post-AGB stars which may have systematically escaped detection in the classical optical surveys carried out so far. These stars may only be detectable at infrared wavelengths, and they could be the actual precursors of most PNe in our Galaxy.

Among this hidden post-AGB population, Zijlstra et al. (1989) identified a peculiar, very small group of heavily obscured IRAS sources showing both the characteristics of standard OH/IR stars (a strong infrared emission accompanied by the detection of the OH maser emission at 1612 MHz) and PNe (radio continuum emission at centimeter wavelengths). These sources, called for this reason *OHPNe*, were suggested to represent the ‘evolutionary link’ between OH/IR stars and PNe. In most cases, however, the evolutionary stage of the central star was never confirmed observationally, mainly because of the high extinction affecting the whole nebula, which makes the obtention of a useful spectrum of the central star very difficult. This task is further complicated by the uncertainty in the association between the infrared (IRAS) and the radio continuum source, a consequence of the poor astrometric quality of the IRAS Point Source Catalog (PSC) (as large as 1 arcmin in highly confused,

crowded areas close to the Galactic Center, where most of these sources are located).

With the advent of other, more recent infrared missions like MSX (Egan et al. 2003) and 2MASS (Cutri et al. 2003), the situation has significantly improved and the infrared positions of these OHPN stars can now be determined to an accuracy of a few arcsec in the case of MSX, and to the subarcsec level if they are detected by 2MASS. In addition, with ISO/SWS and Spitzer/IRS spectroscopy we can now study the properties of the dust grains formed in their circumstellar shells. In this letter we present Spitzer/IRS spectra ( $\sim 5\text{--}37\ \mu\text{m}$ ) obtained on a representative sample of galactic ‘OHPNe’ in order to elucidate their nature and evolutionary stage.

## 2. Observations and data reduction

A sample of 5 OHPNe: namely, IRAS 17168–3736, IRAS 17393–2727, IRAS 17418–2713, IRAS 17443–2949 and IRAS 17580–3111 (hereafter I17168, I17393, I17418, I17443 and I17580, respectively), all them extremely bright sources at mid-infrared wavelengths (see Table 1) was selected from the ‘GLMP catalog of IRAS sources with infrared colors similar to those of known PNe’ (García-Lario 1992) and observed by us recently with the Infrared Spectrograph (IRS, Houck et al. 2004) on board the Spitzer Space Telescope (Werner et al. 2004). All of them have been identified as stars showing both OH maser emission at 1612 MHz and radio continuum emission (see Table 2) and thus classified as OHPNe (three of them were indeed already included in the original paper by Zijlstra et al. 1989). The observations were carried out between March and April 2005, in the  $9.9\text{--}37.2\ \mu\text{m}$  range, using the Short-High (SH) and Long-High (LH) modules ( $R\sim 600$ ). Two of the sources in the sample (I17393 and I17580) were also observed at lower resolution with the Short-Low ( $64 < R < 128$  SL;  $5.2\text{--}14.5\ \mu\text{m}$ ) module. Note that for such bright stars it is not possible to perform target acquisition using on-source peak-up (neither peak-up on a nearby source helps) and our astrometric accuracy is actually limited by the MSX accuracy, of the order of  $1.8''$ , which is of the order of (or even worse than) the nominal pointing accuracy of Spitzer ( $\sim 1''$ ). This in principle should be enough to avoid photometric losses when centering the source in the Spitzer apertures, at least at the longer wavelengths. In all cases, it was easy to achieve a S/N larger than 50 over the whole spectral range with just 2 exposure cycles of 6 s in each of the three modules SL, SH, and LH. We started our analysis from the co-added 2-D flat-fielded images (one for each nod position; pipeline version 12.3) which were cleaned from bad pixels. The spectra for each nod position were extracted from the 2-D images, wavelength and flux calibrated using the Spitzer IRS Custom Extractor (SPICE) with a point source aperture. Since no sky (off-position) measurements were taken, the contribu-

tion of the expected background flux through each slit was estimated from the model of Reach and coworkers<sup>1</sup> and subtracted from the SH and LH spectra. For the module SL the two nod positions were previously differenced in order to subtract the sky background. The 1-D spectra were cleaned for residual bad pixels, spurious jumps and glitches, smoothed and merged into one final spectrum per module for each source using the Spitzer contributed software SMART (Higdon et al. 2004).

In general, we found a very good match between the different nod position spectra except at wavelengths longer than  $34 \mu\text{m}$ . This spectral range corresponds to the red end (order 11) of the LH module, affected by a strong noise level, and was for this reason excluded from our analysis. In addition, we found a flux deficit of  $\sim 20\%$  in the SL module spectrum of I17580 with respect to the SH observations of the same source. We attribute this mismatch to the slightly extended nature of I17580 at infrared wavelengths and the different apertures used by these observing modes. This interpretation is also consistent with the extended nature ( $6.7''$ ) of the associated radio continuum emission (see Table 2). At longer wavelengths, however, the absolute flux level of the LH module spectra was found to be  $\sim 10\text{--}15\%$  higher for all the sources in our sample with respect to the corresponding SH module observations. In principle, this effect would be expected in case of the sources being extended. However, we suspect that a systematic effect is affecting our LH data. This is because for I17393 (the other source observed in the SL module) the match between the SL and SH modules is perfect, confirming its point source nature (see Table 2) while the LH observations show a similar flux excess. In addition, the non-variable sources in our sample (I17168, I17393 and I17580; see Sect. 4), show as well LH fluxes which are systematically higher than the MSX and the IRAS ones at this wavelength range while the SH fluxes are in perfect agreement with the photometric data. Thus, we scaled the LH spectra to the SH spectra in order to obtain one final spectrum per source.

### 3. Results

The 5 OHPNe are listed again in Table 2 together with the some additional information available for them in the literature such as the main characteristics of their OH maser and radio continuum emission, or the IRAS variability index, as quoted in the IRAS PSC (Beichman et al. 1988). OHPN stars in our sample are so heavily obscured that they are completely invisible in the optical domain, even at wavelengths below  $3 \mu\text{m}$ . I17580 is the only source in our sample for which a near-IR counterpart (K=9.3) was found in the

---

<sup>1</sup>See <http://ssc.spitzer.caltech.edu/documents/background/>

2MASS catalog. During the observations, Spitzer was pointed to the improved coordinates (with respect to IRAS) quoted in the MSX PSC, except for I17580, for which we used the astrometric information in the 2MASS PSC, accurate to within the subarcsec level. These coordinates are compared in Table 2 with the available OH and radio continuum positions. The OH positions nicely coincide within the errors with the Spitzer ones in all cases, confirming that the OH maser emission is associated with the infrared source. Unfortunately, radio continuum measurements date from more than 10 years ago and in some cases it is not possible to make a proper analysis of the associated astrometric uncertainties, although at least for I17168, I17393 and I17418 the radio continuum positions nicely coincide with the OH and infrared positions within a few arcsec.

The reduced Spitzer/IRS spectra are shown in Fig.1. The O-rich chemistry is confirmed by the simultaneous detection of strong and broad amorphous silicate absorptions at 9.7 and 18  $\mu\text{m}$  (the latter less obvious in I17580 and I17393) in all sources, together with complex crystalline silicate profiles generally attributed to olivine and pyroxenes with various mixtures of Mg and Fe (e.g. those at  $\sim 13\text{--}16$ ,  $\sim 19\text{--}21$ ,  $23\text{--}25$ ,  $26\text{--}28$ , and  $29\text{--}31$   $\mu\text{m}$ ; see Koike et al. 2000). The features are seen either in absorption or in emission with a variety of strengths and at slightly different wavelengths from source to source, depending on the specific chemical composition and size of the dust grains in the circumstellar envelope. In particular, we detect crystalline silicate features in emission at 27.8, 29.3, and 30.5  $\mu\text{m}$  (see Fig.1). The 27.8  $\mu\text{m}$  feature can be attributed to forsterite (a Mg-rich crystalline silicate), while the features around 29.3 and 30.5  $\mu\text{m}$  remain unidentified (Molster et al. 2002). At shorter wavelengths, some of these crystalline features appear in absorption or affected by self-absorption (e.g. those features centred at  $\sim 13.6$ , 14.4, 15.4, 19.5, 20.6, 23.6, and 26.6  $\mu\text{m}$ ), indicating the large optical depth of the circumstellar shell. The 13.6 and 14.4  $\mu\text{m}$  features are clearly detected in I17443, less evident in I17418 and I17168 and not seen in I17580 and I17393. The detection of crystalline silicates in absorption has previously been reported in some other extreme OH/IR stars observed with ISO, such as OH 26.5+0.6 (Sylvester et al. 1999) also shown in Fig.1, for comparison. In addition, other unidentified crystalline silicates may also be present in the spectra of our stars, suggesting that other, more unusual dust species may be present in their circumstellar shells.

We have classified the stars in our sample according to the decreasing strength of the amorphous silicate absorption features at 9.7 and 18  $\mu\text{m}$  (from top to bottom in Fig.1) in what it seems to be an evolutionary sequence. The first three sources in Fig.1; I17443, I17418 and I17168, show spectra which are very similar to those observed in other extreme OH/IR stars (Sylvester et al. 1999), and are dominated by the strong and broad amorphous silicate absorption features at 9.7 and 18  $\mu\text{m}$ , with emerging crystalline silicate emission features which are more prominent at longer wavelengths. The two other sources in Fig.1 I17580

and I17393, are probably in a more evolved stage and show much fainter amorphous silicate absorption features at 9.7 and 18  $\mu\text{m}$ . These sources are peculiar in the sense that they display extremely red colors, indicative of a cool expanding circumstellar shell. I17580 seems to be in a less evolved stage compared to I17393, as suggested by the flux drop observed at 60  $\mu\text{m}$  by IRAS. In contrast, I17393 seems to be more evolved, with cooler dust in the shell as deduced from the IRAS photometry at 60  $\mu\text{m}$  and, more interesting, with a strong [Ne II] nebular emission at 12.8  $\mu\text{m}$  (see Fig.1), suggesting that the onset of ionization has already taken place.

#### 4. Variability analysis

Interestingly, we found a good consistency between the Spitzer/IRS spectra and the photometric flux densities measured at different epochs by IRAS and MSX for I17168, I17393 and I17580, confirming their status of non-variable sources, as expected from their low IRAS variability index (VAR column in Table 2). However, this is not the case of I17418 and I17443, for which the IRAS variability index is indeed higher. These sources seem to be strongly variable and may still be evolving as AGB stars (see Sect. 5). The flux differences between our final Spitzer/IRS spectra (after the correction of the 10–15 % flux excess observed in the LH module) and the large photometric variations observed at different epochs (more than 30 % in flux at 25  $\mu\text{m}$ ), cannot be attributed to color-corrections because in the range of temperatures of the sources in our sample ( $\sim 100\text{--}300$  K) they are always lower than 5 and 15 % for the MSX and IRAS photometry, respectively. A possible contamination of the IRAS fluxes by nearby infrared sources can also be discarded, according to the available information in the IRAS and MSX Point Source Catalogs. The variability status of these two sources is also confirmed by the different flux levels measured in the ISO PHOT-S spectra with respect to our Spitzer spectra at the overlapped wavelength regions (see Fig.1).

#### 5. OHPNe: the high-mass precursors to PNe?

The stars in our sample belong to a small group of O-rich AGB stars characterised by their strong obscuration in the optical, which have recently been suggested to represent the missing population of massive AGB stars in our Galaxy. These are extreme OH/IR stars showing the larger OH expansion velocities ( $V_{exp}(OH) > 12 \text{ km s}^{-1}$ ; see Table 2) and the thicker circumstellar envelopes, being usually invisible in the optical domain, as it is the case of the 5 sources here studied. With ISO only a few other obscured massive O-rich AGB stars were observed. Those sources with available ISO spectroscopy display also strong absorption

bands of amorphous silicates together with crystalline silicate features (see e.g. Sylvester et al. 1999), resembling the OHPNe presented in this paper. Analyzing ISO-SWS spectra, García-Lario & Perea-Calderón (2003) found that dramatic changes occur in the infrared SEDs of these stars during this phase of total obscuration. In the case of massive O-rich AGB stars the strong silicate absorption features at 9.7 and 18  $\mu\text{m}$  are seen first in combination with prominent crystalline silicate features which emerge covering the range from 10 to 45  $\mu\text{m}$ . Later, these features become dominant and are sometimes still observed in more evolved O-rich PNe (Molster et al. 2001). It has been suggested that high temperature crystallization can take place at the very end of the AGB phase as a consequence of the strong mass loss (Waters et al. 1996; Sylvester et al. 1999). Alternatively, low temperature crystallization is also predicted in long-lived circumbinary disks surrounding, leading to a different pattern of crystalline silicates (Molster et al. 1999) not observed in our sources. It should be noted that OHPNe in our sample (specially the non-variable ones) may be already developing strong bipolar post-AGB outflows, as it is also observed in bipolar Type I PNe, and it is likely that a thick circumstellar disk/torus (where the crystallization could take place) is surrounding the central source. Our Spitzer spectra reveals with an unprecedented level of detail and better temporal resolution than previous ISO observations the evolution of the dust features at the precise moment when the transition from the AGB to the post-AGB stage is taking place. We basically observe how the strong amorphous silicate absorption features which are characteristic of AGB stars (see the spectra of I17418 and I17443) disappear in very short timescales (see below) leading to a totally different spectrum dominated by crystalline silicate features (seen either in absorption or in emission depending on the optical depth of the shell at different wavelengths), until the gas in the circumstellar envelope gets ionized as a consequence of the rapid increase of the effective temperature of the central star (as it is the case of I17393).

It is well known that the more massive AGB stars ( $M \gtrsim 4\text{--}5 M_{\odot}$  at solar metallicity) can evolve all the way from the AGB phase to the PN stage as O-rich stars as a consequence of the activation of the so-called “hot bottom burning (HBB)” process (e.g. Mazzitelli et al. 1999), which prevents the formation of C-rich AGB stars. Recently, some of the sources displaying a faint, but still visible optical counterpart, have been observed by us (García-Hernández et al. 2006, 2007) and strong overabundances of lithium and rubidium have been found, confirming their status of HBB AGB stars. If our sources are indeed massive HBB AGB stars, as suggested by the O-rich chemical composition, the strong obscuration and the high expansion velocity observed, we would expect a very fast evolution to the PN stage and thus a young dynamical age for the dust in the envelope. If we perform a simple calculation for I17393 (the most evolved object in our sample which is already surrounded by ionized gas), we found that the short wavelength range of the SED (from 5 to

16  $\mu\text{m}$ ) can be well reproduced by dust emitting at 166 K. By assuming a star’s luminosity of 10,000  $L_{\odot}$  (representative of stars at the tip of the AGB phase), the equilibrium radius of astronomical silicates with a typical grain size of 0.1  $\mu\text{m}$  is found to be  $\sim 0.003$  pc. The expansion velocity (14.6  $\text{km s}^{-1}$  as derived from the OH maser emission) give us a dynamical age of the circumstellar envelope of I17393 of only  $\sim 205$  years. This is consistent with the expected transition time for massive post-AGB stars ( $\sim 100\text{--}1000$  yr for  $M \gtrsim 4 M_{\odot}$ ; e.g. Blöcker 1995), which confirms our hypothesis.

In summary, our observations show that at least three of the observed OHPNe are massive non-variable O-rich stars which have left the AGB very recently. They must be rapidly evolving towards the PN stage representing the evolutionary link between massive OH/IR stars and PNe. The detection of [Ne II] nebular emission in the heavily obscured OHPN star I17393 provides the first observational evidence that the evolution of some of these massive post-AGB stars can be so fast ( $\sim 100\text{--}1000$  yr for  $M \gtrsim 4 M_{\odot}$ ; e.g. Blöcker 1995) that the temperature of the central star may be hot enough to ionize the gas in the circumstellar envelope before it gets diluted into the interstellar medium. For this to happen, the ionization must start within a few hundred years after the AGB mass loss ends. Otherwise, the envelope will have dispersed and the OH emission stopped as it cannot be sustained for too long once the mass loss rate drops by several orders of magnitude at the end of the AGB phase. However, we have also shown here that two of the observed OHPNe are strongly variable O-rich stars and they may still be evolving as AGB stars. At present, the simultaneous detection of radio continuum emission from these sources is not well understood, unless this type of emission has a strong non-thermal contribution which arises from shock interactions at the interface between a recently developed fast wind and previously ejected material. This is supported by the recent detection of strong non-thermal radio continuum emission in the massive ( $M \gtrsim 4 M_{\odot}$ ) O-rich AGB star V1018 Sco (Cohen et al. 2006). We propose that these OHPNe represent the high mass precursors to PNe in the Galaxy.

This work is based on observations made with the Spitzer Space Telescope, which is operated by the Jet Propulsion Laboratory, California Institute of Technology, under NASA contract 1407. JVPC and PGL acknowledge support from grant *AYA 2003–9499 from the Spanish Ministerio de Educación y Ciencia*. MB acknowledges support from Grant 3633 from the Spitzer Space Telescope.



## REFERENCES

- Beichman, C. A., et al. 1988, IRAS Catalogs and Atlases, Vol. 1
- Blöcker, T. 1995, A&A, 299, 755
- Cohen, M., Chapman, J. M., Deacon, R. M., et al. 2006, MNRAS, 369, 189
- Cutri, R. M., et al., 2003, The IRSA 2MASS All-Sky Point Source Catalog
- David, P., Lesqueren, A. M., & Sivagnanam, P. 1993, A&A, 277, 453
- Egan M. P., et al. 2003, Air Force Research Laboratory Technical Report, 2003-1589
- García-Hernández, D. A., García-Lario, P., Plez, B., et al. 2006, Science, 314, 1751
- García-Hernández, D. A., García-Lario, P., Plez, B., et al. 2007, A&A, 462, 711
- García-Lario, P. 1992. Ph.D. Thesis, La Laguna University
- García-Lario, P., et al. 1997, A&AS, 126, 479
- García-Lario, P., & Perea Calderón, 2003, in *Exploiting the ISO Data Archive. Infrared Astronomy in the Internet Age*, p. 97
- García-Lario, P. 2006, in “*Planetary Nebulae in our Galaxy and Beyond*” Eds. M.J. Barlow & R.H. Mendez, Publ.A.S.P., Cambridge Univ. Press, pp. 63
- Houck, J. R., Appleton, P. N., Armus, L. et al. 2004, ApJS, 154, 18
- Hu, J. Y., te Lintel Hekkert, P., Slijkhuis, F., et al. 1994, A&AS, 103, 301
- Higdon, S. J. U., Devost, D., Higdon, J. L., et al. 2004, PASP, 116, 975
- Koike, C., Tsuchiyama, A., Shibai, H., et al. 2000, A&A, 363, 1115
- Kwok, S. 2000, *The Origin and Evolution of PNe*, Cambridge University Press
- Mazzitelli, I., D’Antona, F., & Ventura, P. 1999, A&A, 348, 846
- Molster, F. J., Yamamura, I., Waters, L. B. F. M., et al. 1999, Nature, 401, 563
- Molster, F. J., Lim, T. L., Sylvester, R. J., et al. 2001, A&A, 372, 165
- Molster, F. J., et al. 2002, A&A, 382, 241
- Pottasch, S. R., Bignelli, C., & Zijlstra, A. A. 1987, A&A, 177, L49

- Ratag, M. A., Pottasch, S. R., Zijlstra, A. A., & Menzies, J. 1990, *A&A*, 233, 181
- Ratag, M. A. 1990, Ph.D. thesis, Univ. Groningen
- Sevenster, M. N., Chapman, J.M., Habing, H. J., et al. 1997, *A&AS*, 122, 79
- Suárez, O., García-Lario, P., Manchado, A., et al. 2006, *A&A* 458, 173
- Sylvester, R. J., Kemper, F., Barlow, M. J., et al. 1999, *A&A*, 352, 587
- van Winckel H. 2003, *ARA&A*, 41, 391
- Waters, L. B. F. M., Molster, F. J., de Jong, T., et al. 1996, *A&A*, 315, L361
- Werner, M., Roellig, T. L., Low, F. J., et al. 2004, *ApJS*, 154, 1
- Zijlstra, A. A., Te Lintel Hekkert, P., Pottasch, S. R., et al. 1989, *A&A*, 217, 157
- Zoonematkermani,S., Helfand,D.J., Becker,R.H., et al. 1990, *ApJS*, 74, 181

Table 1. MSX and IRAS photometry

| IRAS Name  | MSX <sub>A</sub><br>(Jy) | MSX <sub>C</sub><br>(Jy) | MSX <sub>D</sub><br>(Jy) | MSX <sub>E</sub><br>(Jy) | IRAS <sub>12</sub><br>(Jy) | IRAS <sub>25</sub><br>(Jy) | IRAS <sub>60</sub><br>(Jy) |
|------------|--------------------------|--------------------------|--------------------------|--------------------------|----------------------------|----------------------------|----------------------------|
| 17168–3736 | 1.79                     | 10.12                    | 23.05                    | 24.95                    | 9.78                       | 37.00                      | 47.90                      |
| 17393–2727 | 0.25                     | 1.05                     | 2.97                     | 10.72                    | 1.83                       | 17.80                      | 36.80                      |
| 17418–2713 | 17.92                    | 29.79                    | 58.00                    | 68.32                    | 14.90                      | 51.30                      | 45.90                      |
| 17443–2949 | 15.11                    | 22.46                    | 42.91                    | 39.45                    | 15.80                      | 39.40                      | 34.50                      |
| 17580–3111 | 1.24                     | 3.62                     | 6.87                     | 13.16                    | 3.23                       | 15.30                      | 7.96                       |

Table 2. The sample of OHPNe and astrometric information<sup>a</sup>.

| Object             | $V_{exp}(\text{OH})^b$<br>(km s <sup>-1</sup> ) | (F <sub>6cm</sub> , Diam.) <sup>c</sup><br>(mJy, ″) | Var | ( $\Delta\alpha$ , $\Delta\delta$ )<br>Spitzer-OH(″) | ( $\Delta\alpha$ , $\Delta\delta$ )<br>Spitzer-Radio(″) |
|--------------------|---|---|-----|--|---|
| 17168 <sup>e</sup> | 13.1 (1)  | (54 <sup>d</sup> , <1) (1)                          | 28  | (+0.75, +0.70)                                       | (+0.45, +3.5)   |
| 17393              | 14.6 (1)  | (1.4, <1) (2)                                       | 18  | (-0.90, +0.40)                                       | (+0.15, -0.10)  |
| 17418              | 15.3 (1)  | (2.0, <1) (3)                                       | 99  | (+1.20, -0.40)                                       | (-4.35, -2.50)  |
| 17443              | ... (2)   | (0.9, 3.4) (4)                                      | 51  | (+0.00, -3.00)                                       | (-7.50, +6.80)  |
| 17580 <sup>f</sup> | 14 (3)  | (2.5, 6.7) (4)                                      | 9   | (+12.0, +0.00)                                       | (-12.00, -30.2)   |

<sup>a</sup>The Spitzer coordinates are taken either from the MSX or the 2MASS Point Source Catalogs (see text ).

<sup>b</sup>References for OH data: (1) Sevenster et al. 1997; (2) David et al. (1993); (3) Hu et al. (1994)

<sup>c</sup>References for radio continuum observations: (1) Zoonematkermani et al. (1990), (2) Pottasch et al. (1987), (3) Ratag 1990, (4) Ratag et al.(1990)

<sup>d</sup>Radio continuum flux at 20 cm (Zoonematkermani et al. 1990)

<sup>e</sup>Improved radio coordinates were taken from the new version of the MAGPIS catalog (<http://third.uclnl.org/gps/>), Robert H. Becker (private communication)

<sup>f</sup>Ziljstra et al. (1989) and Hu et al. (1994) reported a coincidence of the OH position with the infrared one

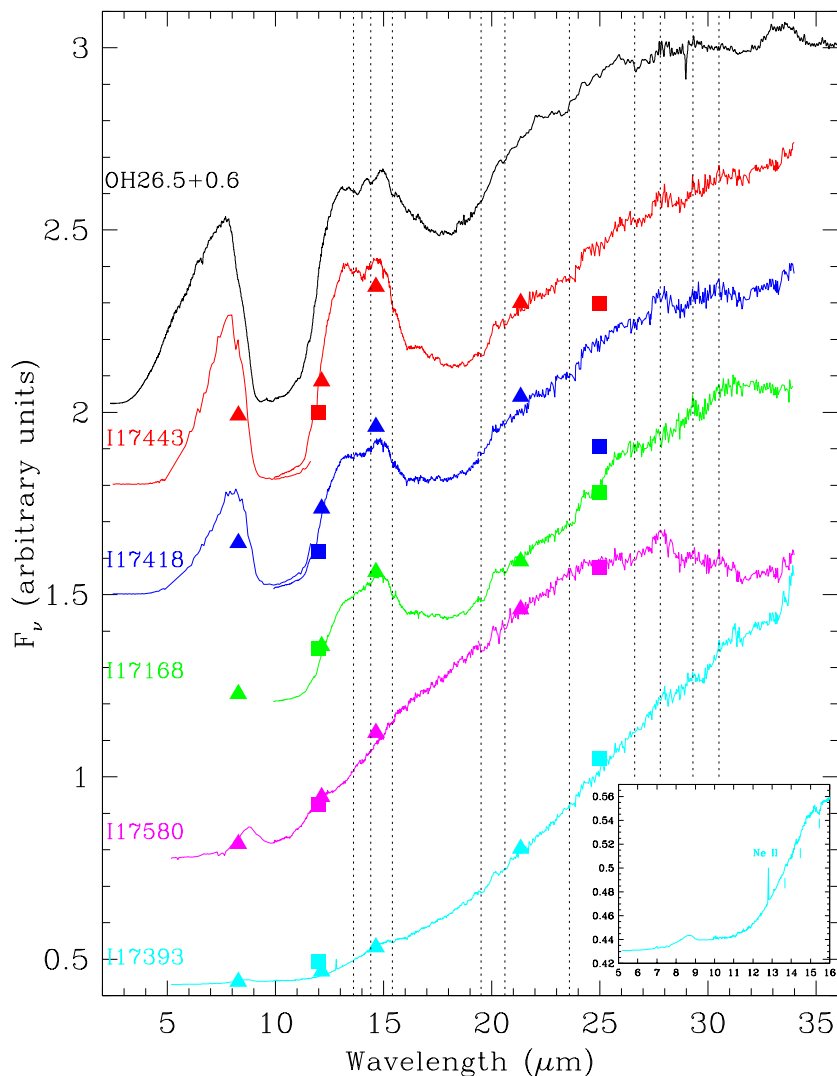


Fig. 1.— The Spitzer/IRS spectra of the 5 OHPN stars observed are shown in comparison to the ISO spectrum of the extreme OH/IR star OH 26.5+0.6 (at the top). MSX (triangles) and IRAS (squares) photometry is also displayed for our target stars. The spectra are shown (from top to bottom) according to the decreasing strength of the amorphous silicate absorption features at 9.7 and 18  $\mu\text{m}$ . The theoretical positions of those crystalline silicate features which appear either in absorption or in emission mentioned in the text are indicated with dashed vertical lines. Note that for I17443 and I17418, the PHOT-S spectra ( $R\sim 90$ ; 2.5–11.6  $\mu\text{m}$ ) available in the ISO Data Archive are also displayed.